

# Improving sulfolane-based electrolyte for high voltage Li-ion cells with electrolyte additives

Jian Xia, J.R. Dahn\*

*Dept. of Physics and Atmospheric Science, Dalhousie University, Halifax, Nova Scotia, B3H3J5, Canada*

---

## H I G H L I G H T S

---

- Sulfolane:ethylmethyl carbonate-based electrolytes with additives are studied.
  -
- 
- 
- 
- 
-

(VC) which showed good cycling and storage performance in NMC442/graphite Li-ion pouch cells. Problems with SL:EMC:VC electrolyte are gas evolution during cycling and storage at high temperatures. Therefore, it is quite crucial and interesting to find electrolyte additives which could function as a gas reducer in SL:EMC electrolytes and, when used together with VC, are competitive or better than state-of-the-art EC-based electrolytes containing electrolyte additives.

Some sulfur containing additives such as prop-1-ene-1,3-sultone (PES) [22,23], methylene methanedisulfonate (MMDS) [24] and trimethylene sulfate (TMS) [25] have been shown to be good gas reducers in NMC111/graphite Li-ion pouch cells. The beneficial effect of these additives is enhanced when combined with a third electrolyte additive, namely, tris(trimethylsilyl) phosphite (TTSPi). Several combinations have shown good storage and cycling performance as well as improved safety features in both NMC111/graphite and NMC442/graphite Li-ion pouch cells [26–28]. Beside these sulfur-containing additives, triallyl phosphate (TAP) was also studied as a good gas reducer at high temperatures in NMC442/graphite pouch cells [29]. When TAP was used together with PES, gas evolution was further decreased while the cycling and storage performance were improved [30].

In this paper, the SL:EMC:VC solvent mixtures with various different electrolyte additives were studied in NMC442/graphite Li-ion pouch cells. Experiments were made using Ultra High Precision Coulometry (UHPC) [31], a precision storage system [32], an *ex-situ* gas evolution apparatus [33] as well as electrochemical impedance spectroscopy (EIS) [34]. Long-term cycling results were also conducted to compare the SL:EMC:VC electrolyte system with EC-based electrolyte systems containing some promising additive blends.

## 2. Experimental

1 M LiPF<sub>6</sub> EC/EMC (3:7 wt% ratio, BASF, 99.99%) was used as the control electrolyte. 1 M LiPF<sub>6</sub> Sulfolane/EMC (3:7 wt% ratio) was used as the studied electrolyte. The sulfolane was obtained from Novolyte Technologies, now BASF (99.99% pure with 9.2 ppm water). The additives were added at 1–8 wt% to the studied electrolyte. These additives included vinylene carbonate (VC), prop-1-ene-1,3-sultone (PES), methylene methanedisulfonate (MMDS), ethylene sulfite (ES), Propanediol cyclic sulfate (trimethylene sulfate - TMS), 1,3,2-dioxathiolan-2,2-oxide (ethylene sulfate - DTD), tris(trimethylsilyl) phosphite (TTSPi) as well as triallyl phosphate (TAP). Fig. S1a (supporting information) shows the chemical structure of additives that were studied in this paper. The reasons for choosing these additives are explained in Refs. [26] and [29]. The purities and the suppliers of the additives used are listed in Table 1 (supporting information). Some promising electrolyte additive combinations in 1 M LiPF<sub>6</sub> EC:EMC (3:7 by wt.) electrolyte include 2% PES + 1% MMDS (or DTD) + 1% TTSPi (PES211) and 2% PES + 2%TAP were also used for comparison in some of the experiments. The details of the PES211 electrolyte have been reported in Ref. [14].

The 402035-size pouch cells employed in this study were all Li [Ni<sub>0.4</sub>Mn<sub>0.4</sub>Co<sub>0.2</sub>]O<sub>2</sub> (NMC442)/graphite cells with a capacity of 245 mAh balanced for 4.7 V operation. Fig. S2 shows SEM images of the top surfaces of the NMC442 and graphite electrodes so that readers can appreciate the morphology of the particles that make up the electrodes. The cells were produced by Li-Fun Technology (Xinma Industry Zone, Golden Dragon Road, Tianyuan District, Zhuzhou City, Hunan Province, PRC, 412000). The pouch cells were vacuum sealed without electrolyte in China and then shipped to our laboratory in Canada. Details about the electrode loadings, thicknesses, compressed electrode density, separator, etc., can be found in Ref. [35].

Before filling with electrolyte, the cells were cut just below the heat seal and dried at 80 °C under vacuum for 14 h to attempt to remove residual water. Then the cells were transferred immediately to an argon-filled glove box for filling and vacuum sealing. The NMC442/graphite pouch cells were filled with 0.75 mL of electrolyte (0.90 g for EC:EMC 3:7 electrolyte and 0.86 g for SL:EMC 3:7 electrolyte). After filling, cells were vacuum-sealed with a compact vacuum sealer (MSK-115A, MTI Corp.). First, cells were placed in a temperature box at 40 °C where they were held at 1.5 V for 24 h, to allow for the completion of wetting. Then, cells were charged at 12 mA (C/20) to 3.5 V. This step is called formation step 1. After Formation step 1, cells were transferred into the glove box, cut open to release any gas generated and vacuum sealed again. These cells were then charged again from 3.5 V at 12 mA (C/20) to 4.5 V. This step is called formation step 2. After formation step 2, the cells were transferred into the glove box, cut open to release gas generated and then vacuum sealed again. These degassing voltages were selected based on the in-situ gas evolution experiments that show most of the gas evolves in the formation step at voltages below 3.5 V and above 4.3 V [36]. After the two degassing processes, cells were then discharged to 3.8 V where impedance spectra were measured.

The cycling/storage procedure was carried out using the Ultra High Precision Charger (UHPC) at Dalhousie University [31]. Testing was between 2.8 and 4.4 V at 40 ± 0.1 °C. Cells were first charged to 4.400 V using currents corresponding to C/10, stored open circuit at 4.400 V for 20.00 h and then discharged to 2.800 V using currents corresponding to C/10. This process was repeated on the UHPC for 15 cycles where comparisons were made. The cycling/storage procedure was designed so that the cells were exposed to higher potentials for significant fractions of their testing time [37]. For storage experiments, cells were first discharged to 2.8 V and charged to 4.5 V two times. Then the cells were held at 4.5 V until the measured current decreased to 0.0025 C. A Maccor series 4000 cyler was used for the preparation of the cells prior to storage. After the pre-cycling process, cells were carefully moved to the storage system which monitored their open circuit voltage every 6 h during a total storage time of 500 h. Storage experiments were made at both 40 and 60 °C.

*Ex-situ* (static) gas measurements were used to measure gas evolution during formation and during cycling [33]. The measurements were made using Archimedes' principle with cells suspended from a balance while submerged in liquid. The changes in the weight of the cell suspended in fluid, before and after testing are directly related to the volume changes through the change in the buoyant force. The change in mass of a cell,  $\Delta m$ , suspended in a fluid of density,  $\rho$ , is related to the change in cell volume,  $\Delta v$ , by

$$\Delta v = -\Delta m/\rho \quad (1)$$

*Ex-situ* measurements were made by suspending pouch cells from a fine wire "hook" attached under a Shimadzu balance (AUW200D). The pouch cells were immersed in a beaker of de-ionized "nanopure" water (18.2 M $\Omega$ ) that was at 20. ± 1 °C for measurement.

Electrochemical impedance spectroscopy (EIS) measurements were conducted on NMC111/graphite pouch cells after formation and also after cycling on the UHPC [34]. Cells were charged or discharged to 3.80 V before they were moved to a 10 ± 0.1 °C temperature box. Alternating current (AC) impedance spectra were collected with ten points per decade from 100 kHz to 10 mHz with a signal amplitude of 10 mV at 10 ± 0.1 °C. A Biologic VMP-3 was used to collect these data.

### 3. Results and Discussion

Fig. 1a–b shows the differential capacity ( $dQ/dV$ ) vs.  $V$  curves for NMC442/graphite pouch cells with some binary and ternary additive combinations in the SL:EMC electrolyte system during formation step 1. From the  $dQ/dV$  vs.  $V$  curves, one can determine at which potential the additives or solvents initially react with the graphite electrode. The control cells (1 M  $\text{LiPF}_6$  in EC:EMC 3:7) showed a pronounced peak at 3.0 V which corresponds to a potential of about 0.65 V vs.  $\text{Li/Li}^+$ . When 2% VC was added to the control electrolyte, the peak shifted to a lower potential of about 2.9 V which corresponds to about 0.75 V vs.  $\text{Li/Li}^+$ . The  $dQ/dV$  vs.  $V$  curve of the cells with 2% VC in SL:EMC system showed a small peak around 2.70 V (0.95 V vs.  $\text{Li/Li}^+$ ). When one more additive was



UHPC cycling.

Fig. 5a–c show a summary of the EIS data after 600 h UHPC cycling at 40 °C (to 4.4 V, including a 20 h storage at 4.4 V each cycle) using the cycle/store protocol, after the 500 h storage test at 60 °C and 4.5 V, and after the 500 h storage test at 40 °C and 4.5 V, respectively. Impedance spectra for all of the cells tested in this study are given in Figs. S6 and S7. Fig. 5, S6 and S7 show that adding more VC to the SL:EMC:2%VC electrolyte system increased the impedance while adding MMDS decreased the impedance. Adding TAP to both SL:EMC and EC:EMC electrolyte systems greatly increased the impedance.

Fig. 6a, b, and 6c show the volume of gas produced during UHPC cycling, during the 500 h storage test at 60 °C and 4.5 V, and during the 500 h storage test at 40 °C and 4.5 V, respectively. Fig. 6a shows that adding more VC to the SL:EMC:2%VC electrolyte system increased the gas evolution. Fig. 6a also shows that cells containing EC:EMC electrolyte produce less gas than the SL:EMC electrolyte system during UHPC cycling. Fig. 6b–c shows that cells containing TAP in both SL:EMC and EC:EMC electrolyte systems had no gas problem at 60 ± 0.1 °C and 40 ± 0.1 °C.

Sulfolane does not form a stable SEI film on the graphite electrode and VC acts as a SEI forming electrolyte additive in the sulfolane:EMC system [21]. When either insufficient or excess VC is present in cells after formation, these cells can generate gas at high potential and at high temperature [22]. That is why the cells described in Fig. 6 all produced a large amount of gas during high temperature storage at 60 ± 0.1 °C except for the TAP-containing cells. It has been proposed that TAP can be easily polymerized at the surface of both graphite and coated NMC442 electrodes [29]. That is presumably why TAP-containing cells have high impedance

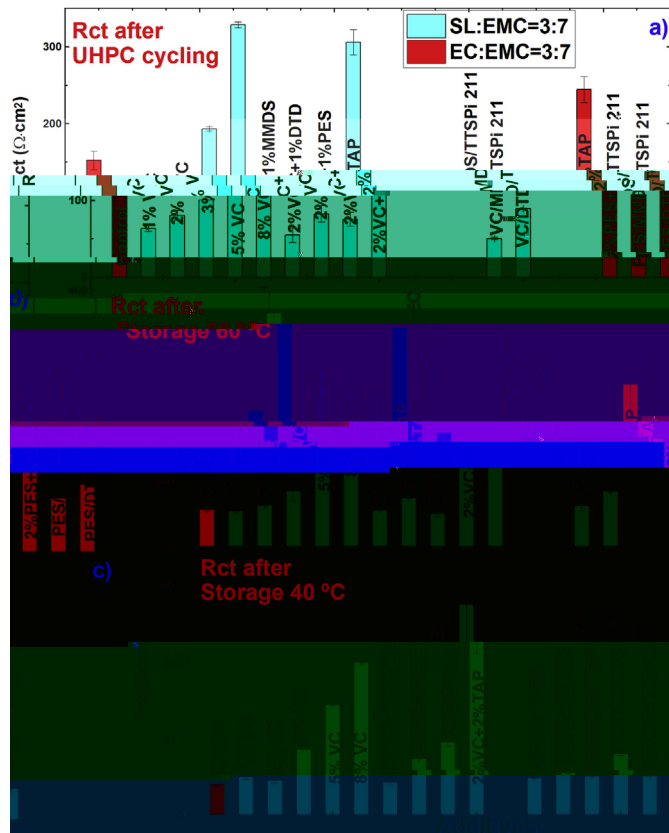


Fig. 5. Summary of the charge transfer resistance ( $R_{ct}$ ) measured after a) UHPC cycling, b) 500 h storage at 60 °C (4.5 V) and c) 500 h storage at 40 °C (4.5 V) for NMC442/graphite pouch cells using SL:EMC electrolyte.

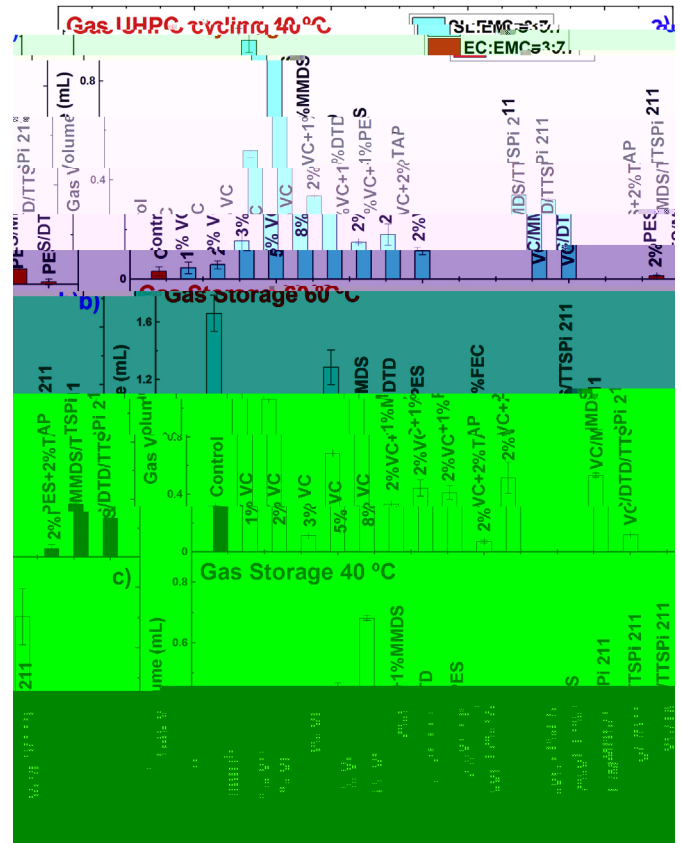


Fig. 6. Summary of the gas evolution measured during a) UHPC cycling, b) 500 h storage at 60 °C (4.5 V) and c) 500 h storage at 40 °C (4.5 V) for NMC442/graphite pouch cells using SL:EMC electrolyte.

at both NMC442 and graphite electrodes, which has been demonstrated by symmetric cell studies in Ref. [29]. The thick SEI films formed by TAP presumably decrease the parasitic electrolyte oxidation reactions between the charged electrode and the electrolyte and therefore decrease gas evolution and improves cycling and storage performance (eg. higher CE, lower charge endpoint capacity slippage during UHPC cycling and lower voltage drop during storage). Ternary additives blends that include VC, a sulfur-containing additive and TTSPi also reduce the rate of parasitic reactions on the positive electrode compared to VC alone, increase the thermal stability of the charged graphite electrode at elevated temperature, improve coulombic efficiency and also reduce impedance of the cells [39]. That may be why such ternary additives blends in the SL:EMC electrolyte perform much better than VC alone in the SL:EMC electrolyte (see Fig. 7). However, these ternary additive blends produce a large volume of gas during high temperature storage, which is the main disadvantage compared to TAP-containing cells in SL:EMC electrolyte.

Fig. 7a, c and e show the capacity vs. cycle number for the NMC442/graphite pouch cells containing different additives combinations in SL:EMC electrolyte. Fig. 7b, d and f show the difference between the average charge and discharge voltage ( $\Delta V$ ) vs. cycle number for the same cells shown in Fig. 7a, c and e, respectively. The long-term cycling cells were the same cells used for the UHPC cycling experiments and the long-term cycling began immediately after the UHPC cycling completed. All cells were continuously cycled with clamps to ensure firm pressure. Cells were cycled between 2.8 V and 4.5 V at 40 ± 0.5 °C using currents corresponding to C/2.5 (100 mA). Only one cell of each type is available due to the



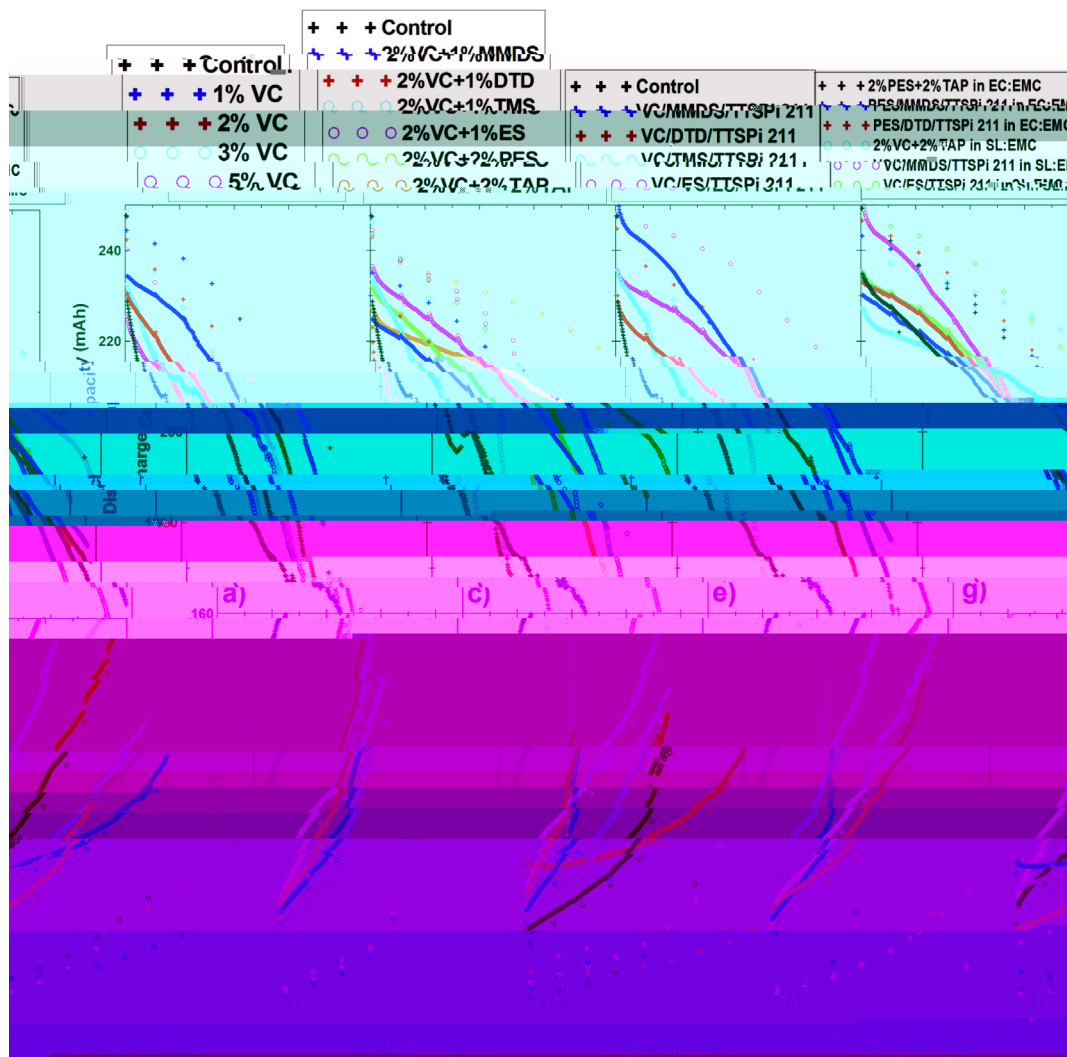


Fig. 7. a, c, e, g) Discharge capacity and b, d, f, h)  $\Delta V$ , all plotted vs. cycle number for NMC442/graphite pouch cells using SL:EMC electrolyte with different additive sets as indicated. “Control” designates cells with 1 M LiPF<sub>6</sub> in EC:EMC 3:7. Panels g and h also contain data for cells with preferred electrolyte additives in EC:EMC. The cycling was between 2.8 and 4.5 V at C/2.4 (100 mA) at 40 ± 0.1 °C.

limited number of testing channels. Fig. 7a–b shows that adding more VC generally leads to worse capacity retention and larger  $\Delta V$  during cycling. Fig. 7b shows adding TAP, ES, MMDS and PES leads to better cycling performance compared to cells containing SL:EMC:2%VC electrolyte. Fig. 7c shows adding TTSPi improves the cycling performance.

In previous studies, “PES-211” [14] and TAP [29] were shown to be beneficial in suppressing impedance growth in NMC442/graphite cells cycled up to 4.5 V. It is therefore meaningful to compare the results in the SL:EMC electrolyte system with results for cells containing “PES-211” or 2% TAP in 1 M LiPF<sub>6</sub> EC:EMC 3:7 electrolyte. Fig. 7g–h compare the discharge capacity as well as  $\Delta V$  vs. cycle number for NMC442/graphite pouch cells containing some of the best additives combinations in SL:EMC:2% VC electrolyte to cells with “PES-211” or 2% PES +2%TAP in EC:EMC 3:7 electrolyte. Fig. 7g–h shows that cells containing 2% VC + 2% TAP in SL:EMC electrolyte have better capacity retention and less impedance growth during long-term cycling than cells with “PES-211” or 2% PES +2%TAP in EC:EMC 3:7. Astute readers may wonder if the improved cycling performance for SL:EMC with 2% VC + 2% TAP is actually caused by the high initial impedance in those cells (see Fig. 7h) which limits reduces the initial capacity and, hence, the

exposure of the positive electrode to the highest potential. However, the storage data shown in Fig. 3a–b do indicate that cells using SL:EMC with 2% VC + 2% TAP do have the best storage performance and hence the smallest rates of electrolyte oxidation which is consistent with a smaller rate of impedance growth as seen in Fig. 7h.

Fig. 8a shows the cycle number when the cell discharge capacity reaches 180 mAh (~80% capacity retention) for NMC442/graphite pouch cells containing different additive combinations in SL:EMC and EC:EMC electrolyte. Fig. 8a shows that all of the SL:EMC-based electrolytes (except 2% VC+1% DTD) have better capacity retention than that of control cells. When compared with additives combinations such as PES 211 and 2% PES +2% TAP in EC:EMC electrolyte, only 2% VC+2% TAP in SL:EMC electrolyte provides better capacity retention. Figs. S8a and S8b (supporting information) show a summary of the gas produced after the entire long-term cycling test and impedance measurement at 3.8 V and at 10. °C after long-term cycling. Fig. S8 shows the additive blends which have better capacity retention generally have excellent gas control and impedance control during long-term cycling. However, 2% VC+2% TAP in SL:EMC electrolyte shows more gas generation and higher impedance than PES 211 and 2% PES +2%TAP in EC:EMC electrolyte after

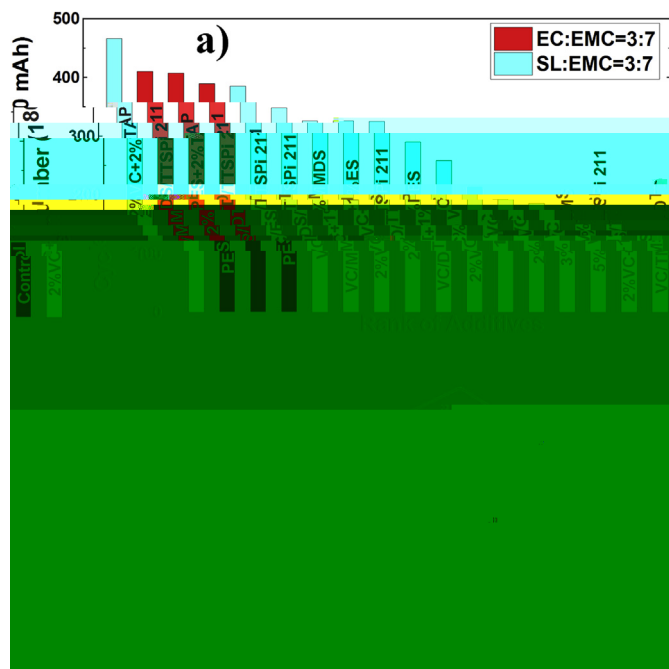


**Fig. 8.** a) The cycle number when the cell capacity reaches 180 mAh (80% retention) for NMC442/graphite pouch cells in SL:EMC electrolyte with different additive sets as indicated. Comparative data for cells with EC:EMC based electrolytes are also shown. The cycle number has been arranged from “best” at the left to “worst” at the right. b) A “radar” or “spider” plot which compares the best additive blends, based on the results in this work, in one graph. The seven axes represent the coulombic inefficiency, the charge endpoint capacity slippage, the charge transfer resistance after UHPC cycling, the gas volume during UHPC cycling,  $V_{drop}$  during storage at 60 °C, the gas volume during storage at 60 °C and the capacity of cycle 400 during long term cycling. The axes have been scaled so that 100% is the value of the additive that has the largest (the worst) value of each parameter. The best additive blend would have values closest to the center of the plot.

the long-term cycling test.

Gas chromatography coupled with a thermal conductivity detector (GC-TCD) was used to analyse the different gases produced during storage. After the storage period, cells were discharged to 3.8 V for EIS measurements. Then cells were stored in a desk drawer at room temperature for about 1 year before the gas compositions were measured. It is very possible that some gases, especially  $\text{CO}_2$  were consumed at the negative electrode during this time in the drawer. Thus, the gas compositions measured may not exactly reflect those in the cell immediately after the 40 °C and 60 °C storage periods. Fig. S9 shows that the main gaseous products during storage at 40 °C include  $\text{H}_2$ ,  $\text{CH}_4$ ,  $\text{CH}_3\text{CH}_3$  and very small amounts of  $\text{CO}_2$ . The production of hydrogen is probably from the reduction of tiny amounts of water originally in the cell.  $\text{CH}_4$  and  $\text{C}_2\text{H}_6$  probably come from the reduction of EMC.  $\text{CO}_2$  probably comes from the oxidation of VC or EMC. At 60 °C, the amounts of  $\text{H}_2$  and  $\text{CH}_4$  were greatly increased. One more gas produced during storage at 60 °C is  $\text{CO}$ , which is likely due to the oxidation of VC or EMC.

Fig. 8b shows a “radar” or “spider” plot which summarizes some of the best electrolyte additive combinations studied in this paper. The seven axes represent the capacity retention at cycle 400, CIE during UHPC testing, charge endpoint capacity slippage during UHPC testing,  $R_{ct}$  after UHPC testing, gas produced during UHPC testing,  $V_{drop}$  during storage at 60 °C (500 h, 4.5 V) and gas evolution during storage at 60 °C. The axes have been scaled so that 100% is the value of the additive that has the largest (the worst) value of each parameter among the 4 electrolytes presented.

Therefore the best additive blend would have values closest to the center of the plot. Fig. 8b shows there is no obvious “winner” in all experiments amongst these additive blends. However, Fig. 8b does show that the cells containing 2% VC+2% TAP in SL:EMC electrolyte have lower CIE, lower charge slippage during UHPC cycling as well as lower gas and lower voltage drop during storage at 60 °C which may contribute to the best capacity retention during long-term cycling. One problem of 2% VC+2% TAP in SL:EMC electrolyte is its high impedance which may limit its high rate cycling performance. Tradeoffs between cycle life time and impedance would have to be made.

### 3.1. Summary and conclusions

SL:EMC:2% VC electrolyte with various additional electrolyte additives combinations was studied in NMC442/graphite pouch type Li-ion cells. The results of CE, charge endpoint capacity slippage, changes in  $\Delta V$  and  $V_{drop}$  during UHPC cycle/store testing to 4.4 V and at 40 °C,  $V_{drop}$  during 500 h storage at 60 °C and 4.5 V, gas evolution, EIS, as well as long-term cycling results were considered and were compared to EC:EMC electrolytes with “PES211” or 2% PES+2%TAP electrolyte additive blends. The results showed that adding more VC, up to 3% VC, to the SL:EMC electrolyte system provided a beneficial effect in decreasing the electrolyte oxidation (lower voltage drop during storage) but adding 3% VC or more dramatically increased cell impedance (Fig. 5) and gassing (Fig. 6). This presumably caused the poor cycling behavior in Fig. 7a for cells with large amounts of VC. The cycling and storage performance of the SL:EMC:2% VC electrolyte system could be improved by adding electrolyte additives, especially 2% TAP. Comparing NMC/graphite cells with EC:EMC electrolyte containing “PES211” or 2% PES +2% TAP additive blends, SL:EMC electrolyte with 2%VC + 2%TAP provided smaller voltage drop during storage, similar CE and lower charge endpoint capacity slippage during UHPC cycling, lower gas evolution during storage at 4.5 V and 60 °C as well as better capacity retention during long-term cycling. However, cells containing SL:EMC electrolyte with 2% VC + 2% TAP display high impedance. This indicates that the SL:EMC:VC:TAP electrolyte system is deserving of further consideration including combinations with a third additive which could serve as an impedance reducer. Such studies are underway in our lab.

### Acknowledgements

The authors acknowledge the financial support of NSERC and 3M Canada under the auspices of the Industrial Research Chairs program. The authors thank Dr. Jing Li of BASF for providing the most of the solvents and salts used in this work.

### Appendix A. Supplementary data

Supplementary data related to this article can be found at <http://dx.doi.org/10.1016/j.jpowsour.2016.06.008>.

### References

- [1] J.B. Goodenough, Y. Kim, *Chem. Mater.* 22 (2010) 587.
- [2] A. Manthiram, *J. Phys. Chem. Lett.* 2 (2011) 176.
- [3] A. Kraysberg, Y. Ein-Eli, *Adv. Energy Mater.* 2 (2012) 922.
- [4] K. Amine, H. Yasuda, M. Yamachi, *Electrochem. Solid State Lett.* 3 (2000) 178.
- [5] J. Wolfenstine, J. Allen, *J. Power Sources* 136 (2004) 150.
- [6] J. Hadermann, A.M. Abakumov, S. Turner, Z. Ha, N.R. Khasanova, E.V. Antipov, G. Van Tendeloo, *Chem. Mater.* 23 (2011) 3540.
- [7] B.H. Huang, S. Yin, T. Kerr, N. Taylor, L.F. Nazar, *Adv. Mater.* 14 (2002) 1525.
- [8] J. Kim, S. Myung, C.S. Yoon, S.G. Kang, Y. Sun, *Chem. Mater.* 16 (2004) 906.
- [9] Z. Lu, D.D. MacNeil, J.R. Dahn, *Electrochem. Solid State Lett.* 4 (2001) A200.
- [10] L. Yang, B. Ravel, B.L. Lucht, *Electrochem. Solid State Lett.* 13 (2010) A95.

- [11] K. Xu, Chem. Rev. 114 (2014) 11503.
- [12] Y. Wang, L. Xing, W. Li, D. Bedrov, J. Phys. Chem. Lett. 4 (2013) 3992.
- [13] L.E. Downie, J.R. Dahn, J. Electrochem. Soc. 161 (2014) A1782.
- [14] L. Ma, J. Xia, J.R. Dahn, J. Electrochem. Soc. 161 (2014) A2250.
- [15] K.J. Nelson, G.L. Eon, A.T.B. Wright, L. Ma, J. Xia, J.R. Dahn, J. Electrochem. Soc. 162 (2015) 1046.
- [16] K. Xu, C.A. Angell, J. Electrochem. Soc. 149 (2002) A920.
- [17] A. Abouimrane, I. Belharouak, K. Amine, Electrochem. Comm. 11 (2009) 1073.
- [18] X. Sun, C.A. Angell, Electrochem. Comm. 11 (2009) 1418.
- [19] J. Xiang, F. Wu, R. Chen, L. Li, H. Yu, J. Power Sources 233 (2013) 115.
- [20] N. Shao, X.-G. Sun, S. Dai, D. Jiang, J. Phys. Chem. B 115 (2011) 12120.
- [21] J. Xia, J. Self, L. Ma, J.R. Dahn, J. Electrochem. Soc. 162 (2015) A1424.
- [22] J. Xia, L. Ma, C.P. Aiken, K.J. Nelson, L.P. Chen, J.R. Dahn, J. Electrochem. Soc. 161 (2014) A1634.
- [23] K.J. Nelson, J. Xia, J.R. Dahn, J. Electrochem. Soc. 161 (2014) A1884.
- [24] J. Xia, N.N. Sinha, L.P. Chen, G.Y. Kim, D.J. Xiong, J.R. Dahn, J. Electrochem. Soc. 161 (2014) 84.
- [25] J. Xia, N.N. Sinha, L.P. Chen, J.R. Dahn, J. Electrochem. Soc. 161 (2013) A264.
- [26] D.Y. Wang, J. Xia, L. Ma, K.J. Nelson, J.E. Harlow, D. Xiong, L.E. Downie, R. Petibon, J.C. Burns, a. Xiao, W.M. Lamanna, J.R. Dahn, J. Electrochem. Soc. 161 (2014) A1818.
- [27] J. Xia, L. Ma, J.R. Dahn, J. Power Sources 287 (2015) 377.
- [28] L. Ma, D.Y. Wang, L.E. Downie, J. Xia, K.J. Nelson, N.N. Sinha, J.R. Dahn, J. Electrochem. Soc. 161 (2014).
- [29] J. Xia, L. Madec, L. Ma, L.D. Ellis, W. Qiu, K.J. Nelson, Z. Lu, J.R. Dahn, J. Power Sources 295 (2015) 203.
- [30] J. Xia, Z. Lu, J. Camardese, J.R. Dahn, J. Power Sources 306 (2016) 516.
- [31] T.M. Bond, J.C. Burns, D. a. Stevens, H.M. Dahn, J.R. Dahn, J. Electrochem. Soc. 160 (2013) A521.
- [32] N.N. Sinha, T.H. Marks, H.M. Dahn, a. J. Smith, J.C. Burns, D.J. Coyle, J.J. Dahn, J.R. Dahn, J. Electrochem. Soc. 159 (2012) A1672.
- [33] C.P. Aiken, J. Xia, D.Y. Wang, D. a. Stevens, S. Trussler, J.R. Dahn, J. Electrochem. Soc. 161 (2014) A1548.
- [34] R. Petibon, C.P. Aiken, N.N. Sinha, J.C. Burns, H. Ye, C.M. VanElzen, G. Jain, S. Trussler, J.R. Dahn, J. Electrochem. Soc. 160 (2012) A117.
- [35] D.Y. Wang, A. Xiao, L. Wells, J.R. Dahn, J. Electrochem. Soc. 162 (2014) A169.
- [36] J. Self, C.P. Aiken, R. Petibon, J.R. Dahn, J. Electrochem. Soc. 162 (2015) A796.
- [37] J. Xia, M. Nie, L. Ma, J.R. Dahn, J. Power Sources 306 (2016) 233.
- [38] J.C. Burns, X. Xia, J.R. Dahn, J. Electrochem. Soc. 160 (2012) A383.
- [39] L. Ma, D.Y. Wang, L.E. Downie, J. Xia, K.J. Nelson, N.N. Sinha, J.R. Dahn, J. Electrochem. Soc. 161 (2014) A1261.